An ISO 26262 compliant built-in self-test for 77 GHz automotive radar sensors

Raik Schnabel
Engineering Components Radar
Robert Bosch GmbH
Leonberg, Germany
Email: raik.schnabel@de.bosch.com

Dirk Steinbuch
Engineering Components Radar
Robert Bosch GmbH
Leonberg, Germany
Email: dirk.steinbuch@de.bosch.com

Robert Weigel
Lehrstuhl für Technische Elektronik
University of Erlangen-Nuremburg
Erlangen, Germany
Email: weigel@lte.e-technik.uni-erlangen.de

***Abstract*—More and more applications and a steadily increasing market penetration are showing the success of radar based driver assistance systems. While in recent years most of those systems were focussing on the advance of the drivers' comfort, today many safety applications are offered. As those systems can directly influence the vehicle dynamics, functional safety in terms of new normative requirements, such as the ISO 26262 is gaining more interest. Therefore, in this paper a built-in self-test is presented which is able to monitor multiple receiver paths by measuring the amplitude and phase imbalance among all channels. Four different types of coupling elements to feed a test signal into receiver paths are investigated and evaluated in terms of their precision. Furthermore, a method for a baseband evaluation is proposed.**

***Keywords*—77 GHz, automotive radar, ISO 26262, online monitoring, BIST, built-in self-test**

I. Introduction

Allowing a convenient and safe driving has been the claim of driver assistance systems since the early beginnings. Thereby, radar based systems play a major role in achieving the goal of having road traffic without serious injuries, which since 1997 is often referred to as "Vision Zero". An increasing list of applications [1] and a steadily increasing mass market penetration is underlining this fact. Thereby, a major contribution is surely due the remarkable progress in performance and cost-efficiency during the last years [2]. However, the higher complexity and responsability of such applications is also demanding for a reliable monitoring of critical hardware failures. Until recently, the focus of built-in self-tests (BIST) and online monitoring functions has mostly been on two other aspects. First those functions are implemented to reduce the effort for front-end testing at the end of chip fabrication. Secondly, especially in communications BIST procedures are used to guarantee a high availability by monitoring critical system parameters. With the steadily increasing demand for safety related applications, such as Autonomous Emergency Braking (AEB) or Lane Change Assist (LCA), the development of monitoring functions to expeditiously detect critical hardware failures is gaining momentum.

II. ISO 26262

Furthermore, this trend is driven by normative requirements, especially by the recently released ISO 26262. It has been derived from the IEC 61508 and adapted to the facts of the automotive sector. This has become necessary to reduce the risk of potentially dangerous malfunctions for the rapidly increasing use of safety-relevant application. Besides setting requirements for the development process of such products this standard is requesting for a high hardware monitoring coverage depending on the criticality of the overlying application. Furthermore, it has to be made sure that the failure diagnosis time complies with the fault tolerant time to guarantee that a safe state can be reached before a dangerous system reaction can occur. As a result, current BIST and monitoring concepts have to be reconsidered and complemented by new approaches according to those requirements.

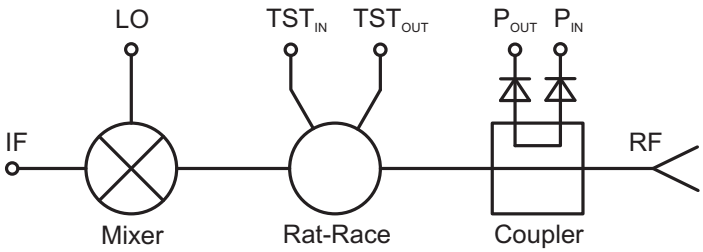

Fig. 1. Receiver path monitoring principles: mixer and antenna matching monitoring using test signals in forward and reverse direction

III. Monitoring Concept

For automotive radar sensors it is crucial to detect failures that can cause an unjustified intervention into the vehicle dynamics. Such reactions can e.g. be triggered by ghost targets, a bad angle estimation or a sudden loss of the tracking of an object. For most sensor concepts the receiving path will be the most critical in order to prevent such dangerous situations. So far, a good part of the receiving path can e.g. be monitored by using a test signal directly fed into the mixer [3].

A missing link of such concepts concerning the functional safety is down to the fact that the receiver path can only be monitored beginning at the on-chip feed point of the test signal (see Figure 1). As a result, the condition of the antenna as well as its interconnection to the MMIC cannot be evaluated. However, this part of the signal path has a major influence on the quality of angle estimation. Although the ISO 26262 is basically focussing on electrical and electronic failures, passives such as bond wires, solder balls or microstrip lines should be considered, if a violation of safety goals could

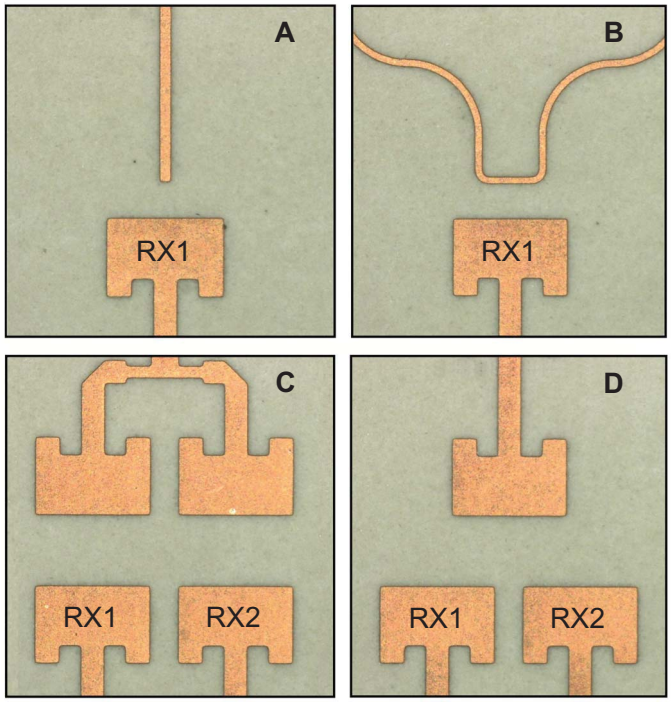

Fig. 2. Investigated approaches for monitoring the amplitude and phase imbalance of various receiver paths using a test signal

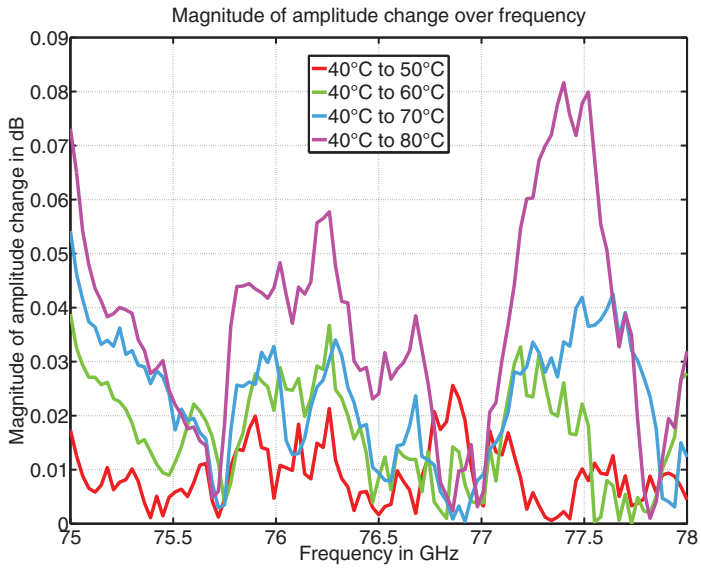

Fig. 3. Magnitude of the amplitude change over frequency for several temperature steps of coupler variant A

arise in case of defects or degradation. A conceivable failure mode is the break of the interconnection between a solder ball and metal layers of the MMIC due to exceeding thermal or mechanical stress. A well-known approach to detect such failures is to determine the matching by measuring the forward and reverse power using on-chip power sensors. However, at least for bistatic concepts this would require another RF test signal to be fed in the receive path in transmitting direction. Furthermore, especially failures at the transition will more likely result in an unwanted phase shift than in noticeable transmission losses. Hence, in order to achieve a maximum monitoring coverage the determination of the receiving paths' amplitude and phase imbalance is absolutely mandatory.

We propose the following approach to fulfill this requirement. A test signal with an offset frequency in relation to the LO signal is generated and routed on the PCB. Afterwards the signal is symmetrically splitted and fed into all receiving channels to be monitored. In order to cover the whole receiving path the test signal is coupled directly into the antenna elements. Therefore, several coupling structures have been investigated (s. Figure 2). In order to achieve a maximum measurement precision for the receiver paths, the focus of the investigation was on the minimization of the amplitude and phase imbalances of the coupled test signal. Due to the fact, that initial imbalances can be calibrated the major task is to minimize the imbalance which occurs over the relevant temperature range of $-40°C$ to $+85°C$. Considering a perfectly symmetric splitting of the test signal and identical coupling structures, those imbalances should not even occur over temperature variation. However, due to imperfections such as etching tolerances or locally different coefficients of thermal expansion in the PCB they do occur. As this behaviour is hard to predict by 3D EM simulations very different coupling approaches have been chosen. The variants C and D rely on patch to patch coupling, while the variants A and B introduce dedicated structures for monitoring purposes only. The former come with a higher insertion loss of $S_{21} \approx -32dB$ for structure D and $S_{21} \approx -28dB$ for the double patch arrangement of structure C, respectively. However, the coupling is strong enough to cover at least four adjacent receiving patches and therefore allows a higher degree of freedom for designing the actual radiation pattern due to the fact that only one coupling structure needs to be arranged. The achieved results of $S_{21} \approx -24dB$ for variant B are slightly better. However, as the second port of each coupling element needs to be terminated, this variant occupies the largest area on the PCB and reduces the flexibility for the antenna design. Finally, variant A achieved the lowest insertion loss of $S_{21} \approx -21dB$, as it can be placed closer to to the receiving element without influencing the actual radiation pattern. However, as the matching for a stub line is very poor, the layout of the distribution network for multiple receiver paths has to be considered carefully. In order to determine the imbalance over temperature for all structures, 3-port measurements using a network analyzer have been carried out. Therefore two receiving paths of each variant have been connected to a T-junction on the PCB. The common LO port was fed by a sweeper which was synchronized with the VNA using a 10 MHz reference clock. It was followed by a frequency doubler and contacted using a coplanar GSG probe. Both RX ports were also contacted using coplanar probes and connected to the VNA using millimeter wave test modules. The temperature has been stepped from $40°C$ to $80°C$ in order to avoid imprecisions due to vibrations introduced at lower temperatures by the flow of the cooling fluid underneath the chuck.

Figures 3 and 4 show the amplitude and phase imbalance for coupler variant A with the stub line being $100\mu m$ wide and $300\mu m$ away from the receiving patch. When considering

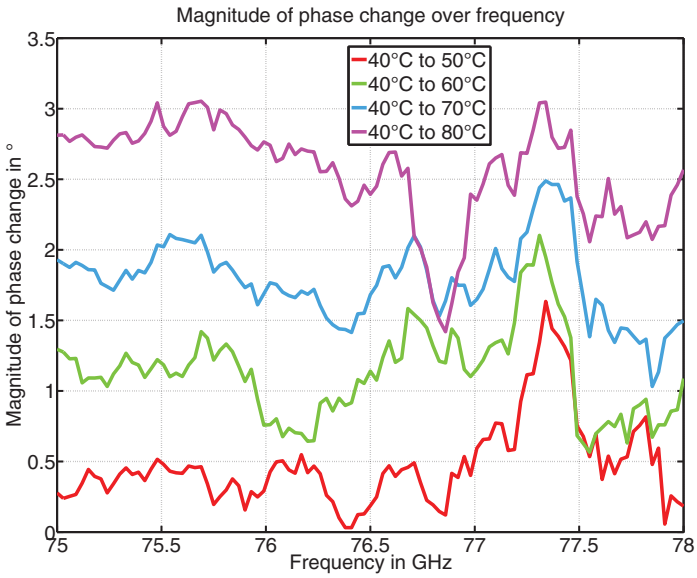

Fig. 4. Magnitude of the phase change over frequency for several temperature steps of coupler variant A

Coupling element	S_A in dB/K	S_ϕ in $^\circ/K$
Variant A	0.0020	0.078
Variant B	0.0074	0.055
Variant C	0.022	0.14
Variant D	0.025	0.12

TABLE I. MEASUREMENT IMPRECISION OF INVESTIGATED COUPLER ELEMENTS DUE TO TEMPERATURE EFFECTS

the maximum changes for each temperature step the amplitude and phase sensitivities for each variant can be obtained. For most of the structures this behaviour was nearly linear as to be expected due to the linearity between temperature and thermal expansion. However, for structures which have been located too close to the receiving antenna even a non-monotonic relation has been observed. Hence, those structures have been excluded for the evaluation of the different coupler types. Table I illustrates the averaged measured sensitivities for each coupler variant. When considering an initial calibration at room temperature the maximum measurement imprecision for the amplitude and phase imbalance of the receiver paths can be obtained by multiplying the sensitivities by $65°C$ ($-40°C$ to $25°C$).

IV. BASEBAND EVALUATION

The test signal being fed into the receiving antennas by the coupling elements is down-converted to a zero-IF frequency. The monitoring of all receiver paths is then applied by the evaluation of amplitude and phase at the IF frequency of the test signal. Therefore, an A/D conversion and a FFT calculation are carried out prior to this step. In order to measure the amplitude and phase imbalance among all receiver channels a precise and robust figure of merit needs to be defined. In the easiest way the measured amplitudes can individually be compared against a generic threshold level valid for every sensor. However, according to Figure 5 this might not be very accurate due to manufacturing tolerances of all involved components, especially of the MMICs. As a result, a constant threshold would necessarily have to be placed considerably

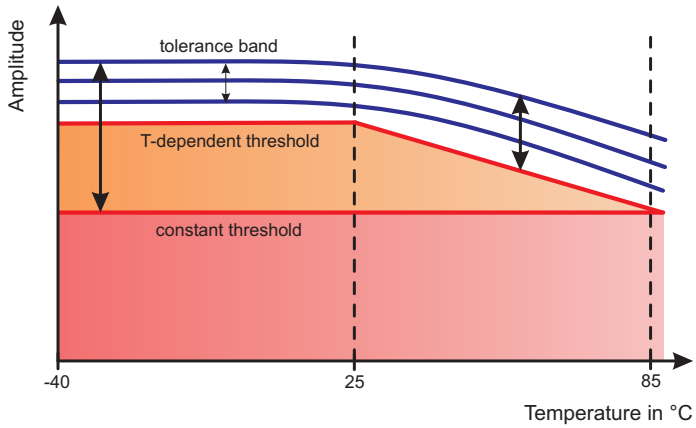

Fig. 5. Schematic of threshold levels for a receiver path monitoring using a test signal: lack of precision for generic threshold levels (constant / temperature-dependent) due to a temperature-dependency of the test signal amplitude and manufacturing tolerances

below the expected tolerance band. Otherwise manufacturing tolerances would directly lead to an unacceptably high false alarm rate. Furthermore, an influence of the temperature on the amplitudes of the test signal has to be considered due to the temperature dependency of the mixer gain and the test signal output. In the test setup using a 77 GHz four-channel eWLB packaged receiver [4] a total temperature variation of about $3-5dB$ has been measured. This can be overcome by implementing a temperature dependent threshold level. However, depending on the accuracy of on-chip temperature measurements and tolerances a sensor individual calibration can be mandatory, which in turn increases the manufacturing effort due to required conditioning steps.

Therefore a different approach has been chosen here. Instead of comparing all amplitudes against a constant threshold level, the amplitudes of all receiver channels are considered relatively. Due to the fact that typically the variation in signal amplitude among all channels is much lower than between different sensors, a relative evaluation allows for a finer resolution to detect power drops. Our proposed figure of merit is the standard deviation of the test signal amplitudes of all n channels. When considering a defect in only one channel, the variance in the faultless case σ_f^2 can be decomposed as follows:

$$\sigma_f^2 = \left(\frac{1}{n-1}\right) \cdot \left[(x_{n,f} - \mu_f)^2 + \sum_{i=1}^{n-1} (x_{i,f} - \mu_f)^2\right] \quad (1)$$

In case of a defect with a signal drop d the variance σ_d^2 results to:

$$\sigma_d^2 = \left(\frac{1}{n-1}\right) \cdot \left[(x_{n,d} - \mu_d)^2 + \sum_{i=1}^{n-1} (x_{i,d} - \mu_d)^2\right] \quad (2)$$

Thereby the following relations apply:

$$\mu_d = \mu_f - \frac{d}{n} \quad (3)$$

$$x_{n,d} = x_{n,u} - d \tag{4}$$

By comparing the variance in the faultless and in the defect case one obtains the reserve R to allow a unique distinction between both conditions.

$$R = \sigma_d^2 - \sigma_f^2 \tag{5}$$

Setting the reserve to zero results in the maximum inherent imbalance which can be tolerated for a unique detection of a signal drop d. At this condition the following relation holds:

$$x_{n,u} = \mu_{u,n-1} + \frac{d}{2} \tag{6}$$

Insertion of this relation in (1) and further transformation give the minimal threshold level:

$$\sigma_{th,min}^2 = \frac{1}{n} \cdot \left(\frac{d}{2}\right)^2 \tag{7}$$

For the tolerable imbalance a applies:

$$\sigma_{th,min}^2 \geq \sigma_a^2 \tag{8}$$

$$\frac{1}{n} \cdot \left(\frac{d}{2}^2\right) \geq \frac{n}{n-1} \cdot \left(\frac{a^2}{2}\right) \tag{9}$$

As a result, the tolerable amplitude imbalance must hold:

$$a \leq \sqrt{n-1} \cdot \frac{d}{n} \tag{10}$$

Those results are confirmed by a Monte Carlo analysis. It is based on uniformly random distributed amplitudes in an interval a indicating the inherent maximum imbalance among the test signal amplitudes of all channels. After affecting one channel by a power drop d the standard deviation of the amplitudes is recorded for every random combination in the faultless and in the defect case. Figure 6 shows the resulting distributions for both cases. One can clearly see that a power drop of $6dB$ can uniquely be detected in one of four channels for an inherent signal variation of $a = 2.5dB$. Furthermore, it can be shown that a simultaneous power drop in more than one channel can even be detected with a higher confidence level. Therefore, only a simultaneous defect of all receiver channels is not covered by this relative evaluation. This very uncertain case however can coarsely be monitored by using a constant threshold level. The same principle is also applicable to monitor the balance of the test signal phase.

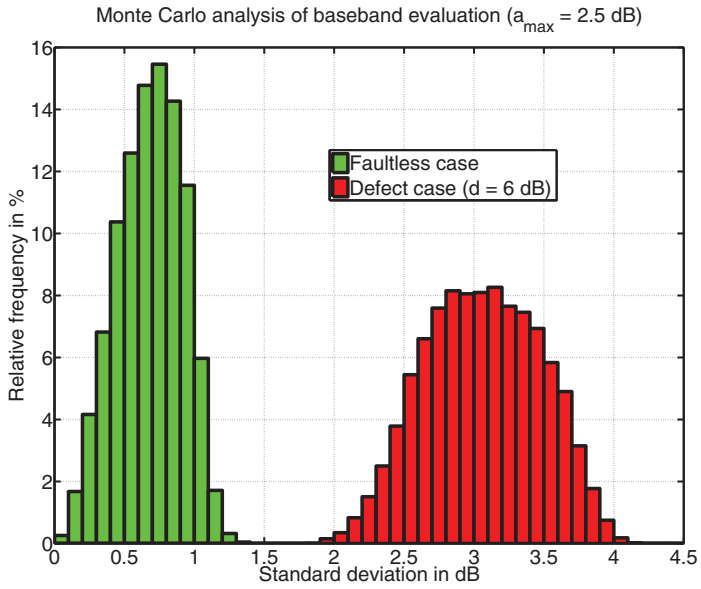

Fig. 6. Monte Carlo analysis of the distributions for the faultless and defect case: A power drop of $6dB$ in one to three out of four channels can uniquely be detected for an inherent amplitude imbalance of $2.5dB$ using the standard deviation as the threshold criterion.

V. Conclusion

A built-in self-test (BIST) able to monitor multiple receiver paths including off-chip antennas has been presented. It is motivated by the need to monitor malfunctions of a radar sensor in order to avoid potentially dangerous driving scenarios when using safety-relevant sensor applications. The BIST is based on the accurate measurement of the amplitude and phase imbalance among various receiver channels to avoid a faulty angle estimation. Therefore, four different types of coupling elements to feed a test signal into the receiving antennas have been investigated in terms of the achievable transmission loss and measurement precision. Assuming an inital calibration at room temperature a precision of $0.13dB$ in amplitude (variant A) and $3.6°$ in phase (variant B) can be achieved. Furthermore, a method to evaluate the quality of various receiver paths at the baseband level has been proposed. Instead of comparing absolute values against a generic threshold, the test signal amplitudes and phases are relatively considered with a higher precision by using their standard deviation.

References

[1] H.-L. Bloecher and J. Dickmann, "Automotive radar for safety and driver assistance applications: Status and trends," in *the European Radar Conference Workshop WFF01*, Oct. 2010.

[2] J. Hasch, E. Topak, R. Schnabel, T. Zwick, R. Weigel, and C. Waldschmidt, "Millimeter-wave technology for automotive radar sensors in the 77 ghz frequency band," *Microwave Theory and Techniques, IEEE Transactions on*, vol. 60, no. 3, pp. 845 –860, march 2012.

[3] D. Kissinger, R. Agethen, and R. Weigel, "Analysis of a built-in test architecture for direct-conversion sige millimeter-wave receiver frontends," in *Instrumentation and Measurement Technology Conference (I2MTC), 2010 IEEE*, may 2010, pp. 944 –948.

[4] C. Wagner, J. Bock, M. Wojnowski, H. Jager, J. Platz, M. Treml, F. Dober, R. Lachner, J. Minichshofer, and L. Maurer, "A 77ghz automotive radar receiver in a wafer level package," in *Radio Frequency Integrated Circuits Symposium (RFIC), 2012 IEEE*, june 2012, pp. 511 –514.